JOURNAL OF MATERIALS SCIENCE 30 (1995) 5427–5432

Thermal behaviours of mechanically alloyed $Ti_{50}Al_{50}$ in a nitrogen atmosphere

K. Y. WANG*
State Key Laboratory for Advanced Metal Materials & Department of Materials Science and Engineering, University of Science and Technology Beijing, 100083 Beijing, People's Republic of China

Thermal behaviours of mechanical alloyed $Ti_{50}Al_{50}$ powders in a nitrogen atmosphere are investigated in this paper. X-ray diffraction and differential thermal analysis were used to determine their characteristics. At the initial milling stage, large amounts of defects were introduced and the grain sizes were gradually refined. The enthalpy changes of formation of γ-TiAl and α_2-Ti_3Al were decreased with increasing milling times. No obvious dissolution of nitrogen into the powder particles occurred at this stage. With increasing milling time, an amorphous phase containing nitrogen gradually occurred. The amorphous phase and small amounts of Ti solid solution were obtained after milling for 30 h in a N_2 atmosphere. The thermal process included two stages. Firstly, the amorphous phase crystallized at low temperature and resulted in the formation of a nanophase; secondly, the grain growth of this nanocrystalline phase occurred at high temperature. The annealing products are different for the milling products obtained at the initial stage (γ-TiAl + α_2-Ti_3Al) and final stage (γ-TiAl + Ti_2AlN), which is attributed to the different nitrogen contents in the milled products. The activation energies for the crystallization and grain growth are 251.9 and 296.9 kJ mol^{-1}, respectively.

1. Introduction

Within the past few years interest has focused on the preparation of amorphous alloys by mechanical alloying. Starting from elemental crystalline powders, a large number of alloy systems, for example Ni–Nb [1], Ni–Ti [2, 3] and several transition-metal–Zr systems [4], have been investigated. Titanium aluminides (α_2-Ti_3Al or γ-TiAl) are very useful structural materials for applications in the aerospace industry owing to their low density, high specific strength and modulus, and good oxidation and corrosion resistance at least up to 800 °C [5, 6]. However, their use has been limited because of poor ductility and fracture toughness at room temperature. To improve these properties, a TiAl compound was recently made as a composite material containing a secondary phase such as boride, carbide, oxide or nitride or crystalline refinement by different methods [7, 8]. Mabuchi *et al.* [7] reported the preparation of composites (γ-TiAl + Ti_2AlN) by combustion reaction. Chang *et al.* [8] reported the preparation of nanocrystalline Ti–Al phase by the inert gas condensation technique. Mechanical alloying has also been used in the investigation of Ti–Al systems [9–14]. More recently, Yamaguchi and Inui mentioned in their review [15] that the drastic reduction of grain size in cast TiAl alloy ingots was obtained by additions of >0.3 wt % N into TiAl alloy and resulted in the improvement of ductility. This also gave another route to improve the mechanical properties of TiAl alloys.

Itsukaichi *et al.* [9, 10] reported the mechanical alloying of Al–Ti systems. The amorphous phase was obtained after milling for 1000 h in an Ar atmosphere. Suryanarayana *et al.* [11] also reported that the amorphous phase could be obtained after milling for 25 h in the Ti–50 at % Al system when a surfactant such as hexane was added during mechanical alloying. Recently, Oehring *et al.* [12] also reported that solid solutions were obtained after mechanical alloying of Ti–Al systems. In previous works [13, 14], we have reported the mechanical alloying of $Ti_{50}Al_{50}$ in a N_2 atmosphere. An amorphous phase containing small amounts of nitride and Ti solid solution was obtained. To the author's knowledge, the thermal behaviour of amorphous Ti–Al systems has not been investigated systematically. In this paper, we will investigate in detail the thermal behaviour of $Ti_{50}Al_{50}$ powders mechanically alloyed in a N_2 atmosphere.

2. Experimental procedures

The milling was performed in a planetary ball mill. Al and Ti powders of a nominal purity of 99.0 and 99.9 at %, and average particle sizes of 60 and 20 μm,

---

*Present address: Department of Chemical and Materials Engineering, University of Kentucky, 177 Anderson Hall, Lexington, KY40506-0046, USA.

0022-2461

respectively, were mixed with a composition of $Ti_{50}Al_{50}$ (atomic ratio). The weight ratio of balls to powders was 60:1. The rate of rotation of the vial was 720 r.p.m. The vial was evacuated first, followed by pouring nitrogen gas into it for each milling process. At selected times, small amounts of ball-milled powders were taken out for analysis. The powders were characterized by the X-ray diffraction (XRD) with CuK_α radiation ($\lambda = 0.154$ nm). The thermal behaviours of the as-milled products were investigated by differential thermal analysis (DTA) using a Perkin-Elmer (model 1700) system. The heating was carried out in a flowing purified argon gas. The measurement of gas content for the final products was made by chemical analysis.

3. Results and Discussion

3.1. X-ray diffraction analysis

X-ray diffraction patterns from the as-milled powders after different milling times in N_2 gas are shown in Fig. 1. Fig. 1a shows the XRD pattern of the powder mixture in the initial state. One can see the existence of crystalline titanium and aluminium diffraction peaks. Fig. 1b shows the XRD pattern for powder milled for 4 h. One can also see the existence of titanium and aluminium diffraction peaks but no nitrides. After milling for 16 h, one finds that the diffraction peaks of titanium and aluminium become broad and weak, and the amorphous phase occurs (see Fig. 1c). From this figure, one also finds the formation of nitride (Ti_2AlN). With further milling up to 30 h, the XRD pattern shows that an amorphous phase and a trace of titanium solid solution are obtained and no nitride appears (see Fig. 1d). The nitrogen content in the final product was about 2.8 wt % N.

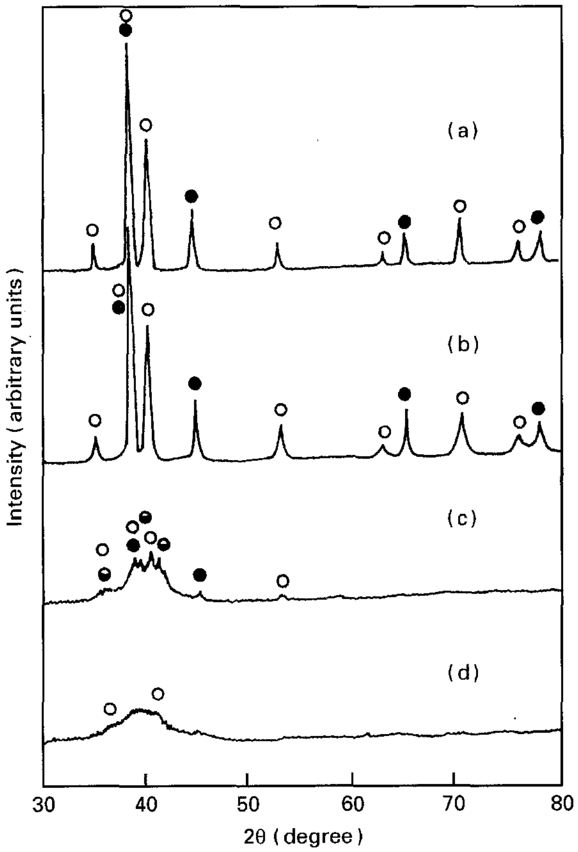

Figure 1 X-ray diffraction patterns of $Ti_{50}Al_{50}$ elemental powders milled in a N_2 atmosphere after (a) 0 h, (b) 4 h, (c) 16 h and (d) 30 h. (○) Ti, (●) Al, (◒) Ti_2AlN.

The amorphous phase can be easily obtained through mechanically alloying (MA) in a N_2 atmosphere when compared with that reported by Itsukaichi *et al.* [9, 10]. In fact, we have performed MA of $Ti_{50}Al_{50}$ in an Ar atmosphere with the same milling conditions [13]. The results showed that an amorphous phase was obtained after milling for 100 h, due to the adherence of Ti and/or Al powders to balls or vial wall which reduced the efficiency of the alloying of the elements. In the present case, nitrogen atoms might have segregated preferentially during the initial milling process, to the grain boundaries of a lamellar structure which is similar to that of mechanically alloyed Cu–Cr in a N_2 atmosphere as reported by Ogino *et al.* [16]. This resulted in the progress of work hardening. Thus, the coalescence of powder particles was hindered and thereby the process of alloying was accelerated. The solid solution of nitrogen in TiAl may play an important role in strain accumulation by hindering defect mobility. As more strain is accumulated in the matrix, the free energy of the system would rise, promoting the formation of an amorphous phase.

3.2. Thermal behaviour analyses of powders milled at different times

DTA curves from the powders milled for 1, 4 and 8 h in a N_2 gas at a heating rate of 20 °C min^{-1} are shown in Fig. 2a. The values of enthalpy changes are shown in Table I. From this figure and Table I, one can observe that the exothermic enthalpy (ΔH_1) became small with increasing milling time. Fig. 3a shows the XRD patterns of as-milled samples (4 h) heated to 600 °C at a rate of 20 °C min^{-1} in the DTA and rapidly cooled to room temperature. The main phases are γ-TiAl phase and α_2-Ti_3Al phase, respectively. Hence, we can infer that the broad exothermic peak (ΔH_1) might be attributed to the formation of intermetallic compounds (γ-TiAl and α_2-Ti_3Al) for the initial milling stage. This also indicates that not enough nitrogen gas permeated into the powder mixtures during the initial milling stage. The intermetallic compounds (γ-TiAl and α_2-Ti_3Al) were directly formed from elemental powder mixtures.

From the DTA curve of powders milled for 1 h, one can see two exothermic peaks. The first exotherm might be due to relaxation effects. The second exotherm might be due to the formation of γ-TiAl and α_2-Ti_3Al phases. From the DTA curve of powders milled for 4 h, one can only see one exothermic peak. This exotherm might be due to the formation of γ-TiAl and α_2-Ti_3Al phases, as indicated in Fig. 3a. We have also noted that the peak reaction temperature of milling for 4 h is lower than that obtained by milling for 1 h. The grain refinement and the introduction of large amounts of defects during MA could result in the decrease of the reaction temperature. After milling for 8 h in N_2 gas, we obtained agglomerates with sizes ranging between 4–6 mm [17]. This indicates that

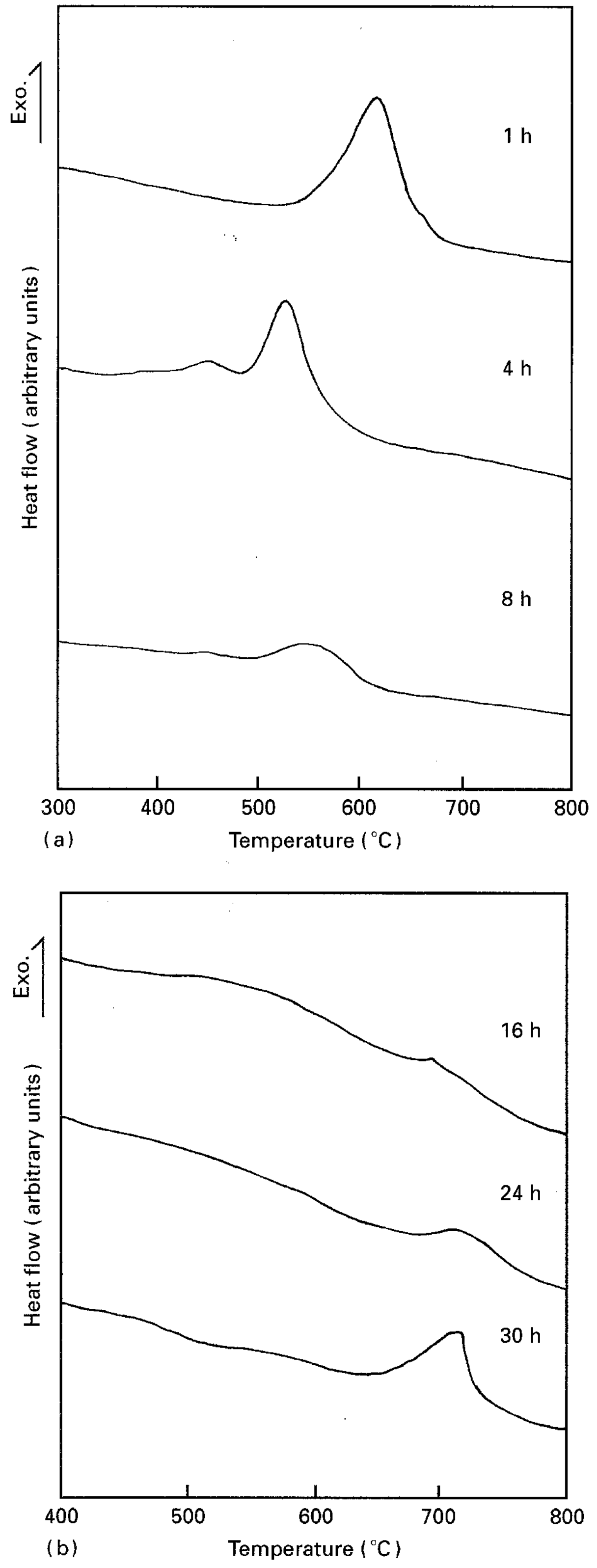

Figure 2 (a) DTA curves of powders as-milled for 1 h, 4 h and 8 h in N_2 gas. (b) DTA curves of powders as-milled for 16 h, 24 h and 30 h in N_2 gas.

a combustion reaction occured, as previosuly reported by one of the authors [17]. The combustion reaction might result in the melting of low melting point metals such as aluminium and this might also result in the increase of crystallite sizes of Ti and Al. Thus, it is reasonable that the peak reaction temperature was higher than that when milling for 4 h in a N_2 gas.

DTA curves from the powders milled for 16, 24 and 30 h in N_2 gas at a heating rate of 20 °C min^{-1} are shown in Fig. 2b. The values of enthalpy changes are also shown in Table I. With increasing milling time the broad exothermic peak mentioned above disappeared, and another significant sharp exothermic peak around 700 °C occurred. From XRD results (see Fig. 1), the amorphous phase gradually formed with increasing milling time. Thus, the main exothermic peaks may be attributed to the crystallization of amorphous phase (see milling for 16, 24 and 30 h, respectively) and the peak crystallization temperature for the powders milled for 30 h in N_2 gas is about 708 °C. With increasing milling time, this exothermic peak becomes more and more pronounced and the values of the thermal enthalpy (ΔH_2) of powders increases, with the value for thermal enthalpy after milling for 30 h being up to 2.10 kJ mol^{-1}.

Fig. 3b shows the XRD patterns of powders as-milled for 30 h in N_2 gas heated to 800 °C at a rate of 20 °C min^{-1} in the DTA and rapidly cooled to room temperature. The main phases are γ-TiAl phase and Ti_2AlN phase, but no trace of α_2-Ti_3Al phase. We can

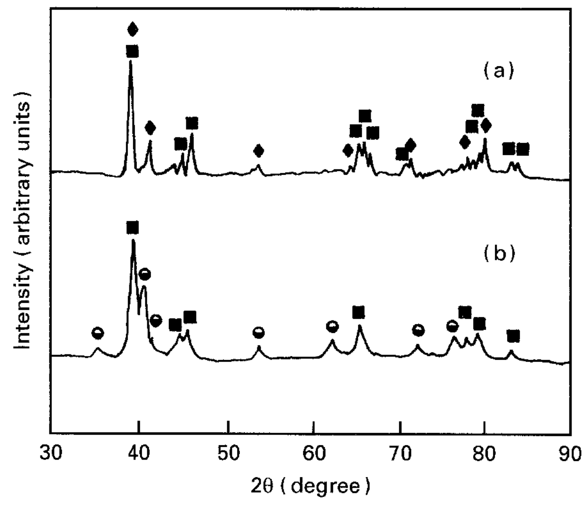

Figure 3 X-ray diffraction patterns of (a) powders as-milled for 4 h in N_2 gas heated at 600 °C at a rate of 20 °C min^{-1} in a DTA and then rapidly cooled to room temperature; (b) powders as-milled for 30 h in N_2 gas heated to 800 °C at a rate of 20 °C min^{-1} in a DTA and rapidly cooled to room temperature. (■) γ-TiAl, (◆) α_2-Ti_3Al, (◒) Ti_2AlN.

TABLE I Thermal enthalpy and peak transition temperature for the powders MA for different times. The heating rate is 20 °C min^{-1}

	MA times (h)					
	1	4	8	16	24	30
ΔH_1 (kJ mol^{-1})	– 19.1	– 14.07	– 9.10	– 6.73	–	–
ΔH_2 (kJ mol^{-1})	–	–	–	– 0.51	– 1.13	– 2.10
T_{p1} (°C)	619.3	547.6	563.9	558.0	–	–
T_{p2} (°C)	–	–	–	689.9	705.4	708.0

infer that the crystallization products were γ-TiAl phase and Ti_2AlN phase for the amorphous phase containing nitrogen. As is well known, the composition of $Ti_{50}Al_{50}$ is the dual phase region containing γ-TiAl and α_2-Ti_3Al. The single γ-TiAl phase region is located in 51 ~ 56 pct Al. At the initial milling stage under a nitrogen gas, a only small amount of N atoms are adsorbed on the surfaces of the powder particles. Therefore, the products after annealing contained only γ-TiAl and α_2-Ti_3Al phases. But with increasing milling times. more and more N atoms dissolved into the powder particles and were accompanied by the solid/solid and/or solid/gas reactions. Thus, it is reasonable that the products after an annealing treatment contained γ-TiAl and Ti_2AlN phases. This is also reflected that the formation of Ti_2AlN phases preceded that the formation of α_2-Ti_3Al phase for the $Ti_{50}Al_{50}$ matrix containing N atoms during the heating process.

From XRD results, we can infer than the solid-state reaction of formation of γ-TiAl can be shown as following:

$$\mathrm{Ti} + \mathrm{Al} \rightarrow \gamma\text{-TiAl} + \alpha_2\text{-Ti}_3\mathrm{Al} + \Delta H_1 \qquad (1)$$

$$\mathrm{Ti} + \mathrm{Al} \rightarrow \text{Amorphous phase} \rightarrow \gamma\text{-TiAl} + \mathrm{Ti}_2\mathrm{AlN} + \Delta H_2 \qquad (2)$$

The values of ΔH_1 and ΔH_2 are shown in Fig. 4. One can see that the values of ΔH_1 decrease and that of ΔH_2 increase with increasing milling time. As is well known, the powder mixtures were mixed completely and formed a layered structure during the initial milling stage. With increasing milling time, the amounts of crystalline phases of Ti and Al decreased. This indicated that the formation of γ-TiAl and α_2-Ti_3Al directly from Ti and Al gradually became impossible, i.e. the values of ΔH_1 became small. At the same time, the amounts of amorphous phase increased with increasing milling time. Therefore, the enthalpy (ΔH_2) for crystallization became large. The result are in good agreement with that of XRD patterns (see Fig. 1). Compared to the result reported by [9, 10], one can see that this amorphous phase is more stable than that of the amorphous phase in [9, 10].

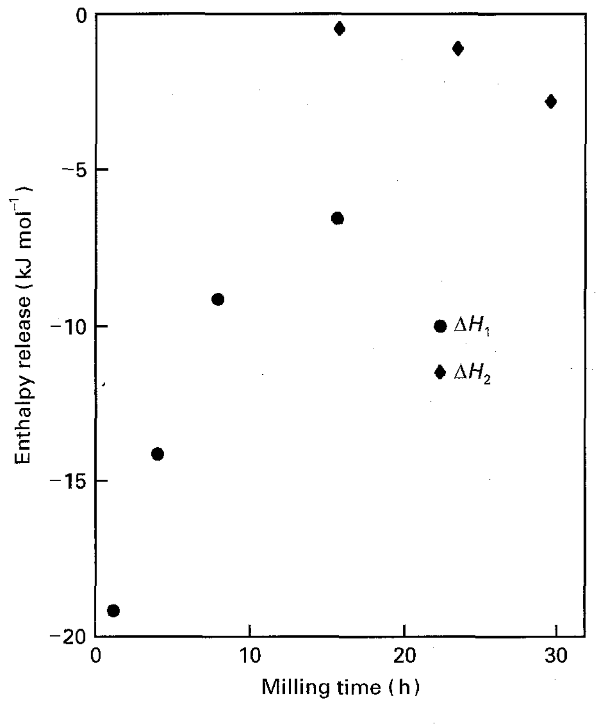

Figure 4 Values of ΔH_1 and ΔH_2 plotted against milling times.

From Fig. 3b, one can find that the main crystallization product is γ-TiAl. The γ-TiAl phase might contain the element nitrogen, which mimics addition of nitrogen into ingots of TiAl alloy [15]. Another product Ti_2AlN might be directly formed from the amorphous matrix. The nitride also might be formed from the titanium solid solution which also contained nitrogen.

From the XRD curve shown in Fig. 3b, one can see that the width of the γ-TiAl diffraction peak is obviously wider than that of the γ-TiAl on the XRD curve shown in Fig. 3a. After milling for 4 h, one can observe that the Bragg diffraction peaks of Ti and Al show almost no distinct changes compared to that of the initial state. So the formation of γ-TiAl directly from the reaction of Ti and Al would not result in the formation of a nanophase. As reported by Yoshizawa *et al.* [19], however, the nanophase could be obtained by "crystallization method" from the amorphous phase. Thus, it is reasonable to expect the formation of nanophase after annealing treatment of the amorphous matrix.

3.3. Analyses of crystallization and grain growth processes of final milled powders

Fig. 5 shows the DTA curves obtained from powders milled for 30 h in N_2 gas at different heating rates

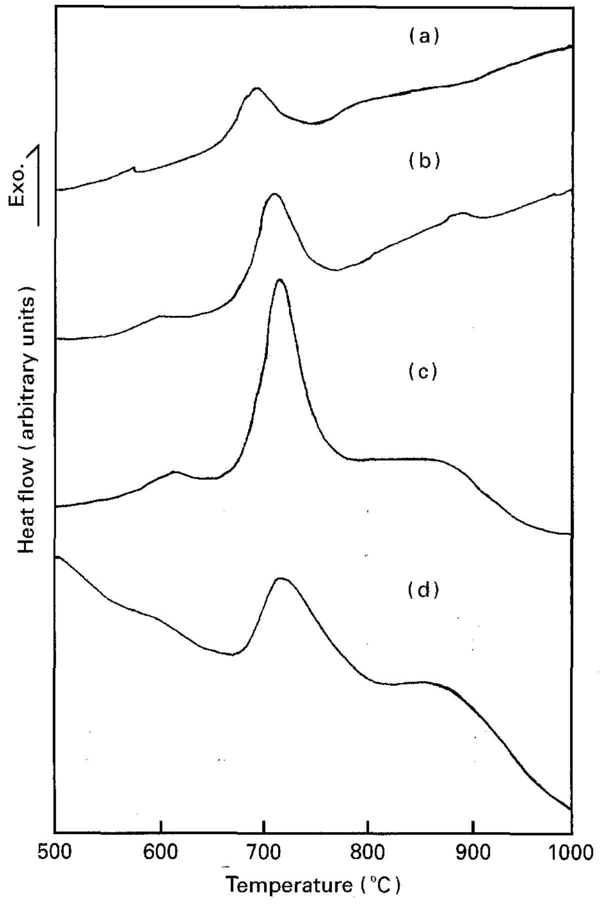

Figure 5 DTA curves of powders as-milled for 30 h in N_2 gas for different heating rates: (a) 10 °C min^{-1}, (b) 20 °C min^{-1}, (c) 40 °C min^{-1} and (d) 80 °C min^{-1}.

(10, 20, 40 and 80 °C min^{-1}). The first sharp exothermic peak temperature for the powders milled for 30 h in N_2 gas is about 708 °C and the value of the thermal enthalpy (ΔH) of powders milled for 30 h is about 2.10 kJ mol^{-1} (for a heating rate of 20 °C min^{-1}). Similar to that shown in Fig. 2b, the temperature measurement range for DTA was up to 1000 °C. One can also see an exotherm at low temperature. This exotherm corresponded to the crystallization of the amorphous phase. It is noted that the second broad exothermic peak appeared in the temperature range 800 ~ 1000 °C for different heating rates. The values of peak temperatures and enthalpy changes of first and second exotherms are shown in Table II. One can see that the enthalpy changes (ΔH_1 and ΔH_2) are not obvious. But the peak temperatures for the first and second exotherms are increasing with increasing heating rates. For the case of heating at 80 °C min^{-1}, one can see that the two exothermic peaks overlapped. We can infer that the first exothermic peak is attributed to the crystallization of the amorphous phase and the second exotherm peak corresponds to the broad exothermic peak at low heating rates. This means that the crystallization temperature increasing with heating rate is higher than that of the second exotherm temperature.

To get more insight into the nature of the two exothermic events we performed annealing experiments for powders milled for 30 h in N_2 gas. For this (Fig. 5d) we heated samples at 80 °C min^{-1} in the DTA to the onset of the first exotherm (about 750 °C) and to 1000 °C, respectively. After heating to these temperatures the samples were rapidly cooled in the DTA and investigated at room temperature by X-ray diffraction. The results are shown in Fig. 6. Fig. 6a shows the XRD pattern of an annealed sample heated to 750 °C, for which the Bragg diffraction peaks of γ-TiAl and Ti_2AlN are very broad. This indicates that the crystallite sizes are in the nanometre range. Fig. 6b shows the XRD pattern of the annealed sample heated to 1000 °C, for which the Bragg diffraction peaks of γ-TiAl and Ti_2AlN became sharp. This indicates that the crystallite sizes increased after this treatment. This also suggested that the second exothermic peak overlapping the first exothermic peak in Fig. 5d can be attributed to the growth of nanocomposites.

So we can describe the crystallization process and grain growth process during heating the sample after milling for 30 h in N_2 gas. Below 800 °C, we can obtain nanocomposites containing γ-TiAl and Ti_2AlN. With increasing annealing temperature, the grains grow rapidly. Thus, if we adjust the annealing temperature and annealing time, we can obtain the nanocomposites of γ-TiAl and Ti_2AlN [13]. Chang *et al.* [8] reported thermal behaviour of nanophase Ti–Al in the range of room temperature ~600 °C by DSC. They also observed that the crystallite size increased sharply when annealed at 900 °C for 2 h. In our experiment, we observed the second exothermic peak around 850 °C and the second exotherm was attributed to the grain growth of the nanocrystalline phase. Detailed analysis is in progress [17].

TABLE II Thermal enthalpy and peak transition temperature for the powders MA for 30 h at different heating rates

	Heating rate (°C min^{-1})			
	10	20	40	80
ΔH_1 (kJ mol^{-1})	– 1.96	– 2.10	– 2.03	–
ΔH_2 (kJ mol^{-1})	– 0.64	– 0.57	– 0.64	–
T_{p1} (°C)	688.7	706.8	727.6	756.4
T_{p2} (°C)	825.8	858.9	880.4	898.6

The apparent activation energy for the overall transformation was determined by the Kissinger–Baswell method [20, 21]:

$$\ln(\Phi/T_p) = -(E_a/RT_p) + \text{constant} \quad (3)$$

where Φ is the heating rate, T_p is the peak temperature, R is the gas constant and E_a is the apparent activation energy indicating the sensitivity of the reaction (transformation) to temperature. The result for powders milled for 30 h in N_2 gas at different heating rates (10, 20, 40 and 80 °C min^{-1}) is shown in Fig. 7, in which the activation energy for the crystallization process is

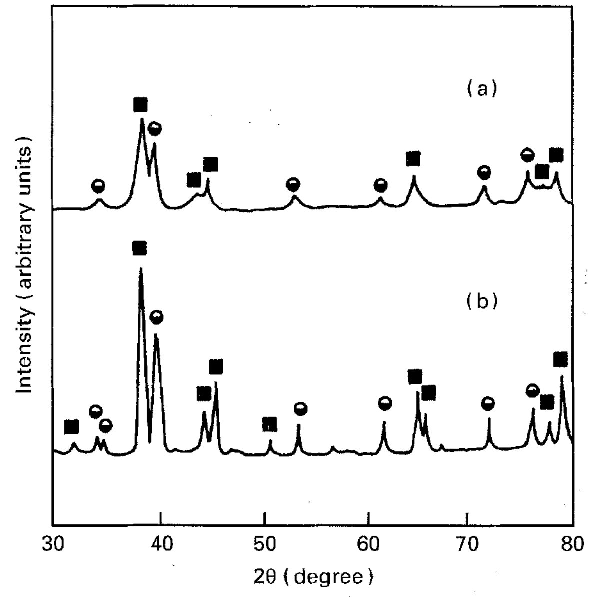

Figure 6 X-ray diffraction patterns for $Ti_{50}Al_{50}$ after milling for 30 h in N_2 gas and subsequent heating at a heating rate of 80 °C min^{-1} in a DTA to different temperatures. After heating to the indicated temperatures the samples were quickly cooled to room temperature for X-ray analysis. (a) Heated to 750 °C and (b) heated to 1000 °C. (■) γ-TiAl, (⊖) Ti_2AlN.

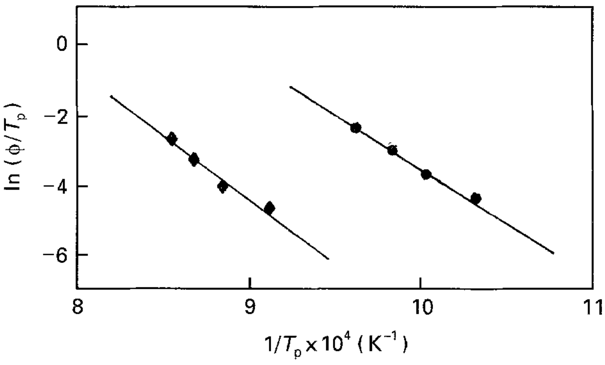

Figure 7 Kissinger plots of the crystallization and grain growth temperatures for $Ti_{50}Al_{50}$ elemental powders milled in a N_2 atmosphere for 30 h. (●) first peak, (◆) second peak.

around 251.9 kJ mol^{-1}. From Fig. 5 and 6, one can find that the second exothermic peak is attributed to the grain growth of the nanocrystalline phase. Thus, the activation energy for the grain growth process can also be calculated, and is about 296.9 kJ mol^{-1}.

4. Conclusion

Mechanical alloying of $Ti_{50}Al_{50}$ in a N_2 atmosphere was investigated in this paper. From the above results, we can obtain these conclusions:

1. During the initial milling stage, large amounts of defects were introduced and the grain sizes were gradually reduced. The enthalpy changes of formation of γ-TiAl and α_2-Ti_3Al were decreased with increasing milling times. No obvious dissolution of nitrogen into the powder particles occurred at this stage.
2. Subsequently, an amorphous phase containing nitrogen can be obtained after 30 h of milling in a N_2 atmosphere. The peak crystallization temperature is 708 °C at a heating rate 20 °C min^{-1} and the activation energy for the crystallization is around 251.9 kJ mol^{-1}. Annealing treatment resulted in the crystallization of the amorphous phase and the formation of a nanophase. Further annealing treatment could result in the grain growth of this nanocrystalline phase. The peak temperature is around 850 °C and the activation energy for the grain growth is about 296.9 kJ mol^{-1}.
3. The annealing products are different from the milling products of the initial stage (γ-TiAl + α_2-Ti_3Al) and the final (γ-TiAl + Ti_2AlN). The enthalpy changes of formation of the intermetallic compounds decreased but the enthalpy changes of crystallization of the amorphous phase increased with increasing milling times.

Acknowledgements

This work was supported by the National Nature Science Foundation of China (No. 59301003) and was partly supported by the Postdoctoral Science Foundation of the Department of Metallurgical Industry, China. The author also acknowledges the financial support by the State Key Laboratory of RSA, Institute of Metal Research, Academia Sinica, Shenyang.

References

1. C. C. KOCH, O. B. CAVIN, C. G. McKAMEY and J. C. SCARBROUGH, *Appl. Phys. Lett.* **43** (1983) 1017.
2. R. B. SCHWARZ, R. R. PETRICH, and C. K. SAW, *J. Non-Cryst Solids* **76** (1985) 281.
3. K. Y. WANG, T. D. SHEN, J. T. WANG and M. X. QUAN, *Scripta Metall. Mater* **25** (1991) 2227.
4. E. HELLSTERN and L. SCHULTZ, *Phi. Mag.* **B56** (1987) 443.
5. F. H. FROES, C. SURYANARAYANA and D. ELIEZER, *J. Mater Sci.* **27** (1992) 5113.
6. S. H. WHANG, C. T. LIU, D. P. POPE and J. O. STIEGLER (eds), "High temperature aluminides and intermetallics" (Metallurgical Society of AIME, Warrendale, PA, 1990).
7. H. MABUCHI, H. TSUDA, Y. NAKAYAMA and E. SUKEDAI, *J. Mater. Res.* **7** (1992) 894.
8. H. CHANG, C. J. ALTSTETTER and R. S. AVERBACK, *ibid.* **7** (1992) 2962.
9. T. ITSUKAICHI, S. SHIGA, K. MASUYAMA, M. UMEMOTO and I. OKANE, *Mater. Sci. Forum* **88–90** (1992) 631.
10. T. ITSUKAICHI, K. MASUYAMA, M. UMEMOTO, I. OKANE and J. G. CABAÑAS-MORENO, *J. Mater. Res.* **8** (1993) 1817.
11. C. SURYANARAYANA, GUO-HAO CHEN, ABDUL-BASER FREFER and F. H. FROES, *Mater. Sci & Eng.* **A158** (1992) 93.
12. M. OEHRING, T. KLASSEN and R. BORMANN, *J. Mater. Res* **8** (1993) 2819.
13. G. CHEN and K. WANG, in "Proceedings of the 2nd International Conference on Structural Application of Mechanical Alloying", edited by J. J. deBarbadillo, F. H. Froes and R. Schwarz ASM, Materials Park, OH (1993), p. 149.
14. K. Y. WANG, G. L. CHEN and J. G. WANG, *Scripta Metall. Mater.* **31** (1994) 87.
15. MASAHARU YAMAGUCHI and HARUYUKI INUI, in "Structural metallics", edited by R. Darolia, J.J. Lewandowski, C.T. Liu, P.L. Martin, D. B. Mircle and M.V. Nathal (The Minerals, Metals & Materials Society, 1993) p. 127.
16. Y. OGINO, T. YAMASAKI, M. MIKI, N. ATSUMI and K. YOSHIOKA, *Scripta Metall. Mater.* **28** (1993) 967.
17. K. Y. WANG, to be published.
18. K. Y. WANG, A. Q. HE and J. T. WANG, *Metall. Trans.* **24A** (1993) 225.
19. Y. YOSHIZAWA, S. OGUMA and K. YAMAUCHI, *J. Appl. Phys.* **64** (1988) 6044.
20. H. E. KISSINGER, *Anal. Chem.* **26** (1957) 1702.
21. P. G. BOSWELL, *J. Thermal. Anal.* **18** (1980) 353.

Received 12 January
and accepted 11 May 1995